NTNU
Kunnskap for en bedre verden

Department of Mathematics

TMA4212 Numerical solution of differential equations by difference methods

Project 2

Author:
Gard Westrum Gravdal, Marcus Hjørund, Simen Lunde Wold

Date: 26.03.2023

Table of Contents

List of Figures

1 Introduction

In this project we consider a model for a convective and diffusive substance in 1d in the stationary regime, e.g. the transport/mixing/decay of a chemical in a fluid moving in a finite tube. Our model is a boundary problem for a Poission like equation:

$$-\left(\alpha u_x\right)_x + \left(bu\right)_x + cu = f(x) \qquad \text{in} \qquad \Omega = (0,1)\,, \tag{1}$$

2 Part 1: A 1d stationary convection diffusion problem

Here we assume $\alpha(x) \geq \alpha_0 > 0$, $c > 0$, $\|\alpha\|_{L^\infty} + \|b\|_{L^\infty} + \|c\|_{L^\infty} + \|f\|_{L^2} \leq K$, and in addition Dirichlet boundary conditions $u(0) = u(1) = 0$.

2.1 Deriving a weak formulation

In the next section we want to show that for any test function $v(x)$, any classical solution $u(x)$ satisfies

$$a(u,v) = F(v) \quad \forall \quad v \in H_0^1\,(0,1)\,, \tag{2}$$

where $a(u,v)$ is a bilinear and continuous function on $H^1 \times H^1$ and $F(v) : H^1 \mapsto \mathbb{R}$ is a linear continuous functional on $H^1(0,1) := \left\{g : g, g_x \in L^2(0,1)\right\}$.

We derive $a(u,v)$ by multiplying (1) by a test function v and taking the integral $\int_0^1 dx$ on both sides. We obtain the weak formulation by taking integration by parts on the two first terms on the left hand side.

$$\int_0^1 -\underbrace{(\alpha u_x)_x v}_{1.} + \underbrace{(bu)_x v}_{2.} + cuv dx = \int_0^1 fv dx, \quad \textit{i.b.p.}: \tag{3}$$

1. $-\int_0^1 (\alpha u_x)_x v\, dx = -\underbrace{[\alpha u_x u]_0^1}_{=0} + \int_0^1 \alpha u_x v_x\, dx = \int_0^1 \alpha u_x v_x\, dx$

2. $\int_0^1 (bu)_x v\, dx = \underbrace{[buv]_0^1}_{=0} - \int_0^1 buv_x\, dx = -\int_0^1 buv_x\, dx$

$$\Rightarrow \quad a(u,v) := \int_0^1 \alpha u_x v_x - buv_x + cuv\, dx = F(v) := \int_0^1 fv\, dx \quad \forall \quad v \in H_0^1(0,1). \tag{4}$$

which is well defined for $u, v \in H_0^1(0,1)$ and $\alpha, b, c \in L^2$.

Next we want to show that $a(u,v)$ is a bilinear and continuous function on $H^1 \times H^1$. Linearity follows straight from the linearity of integrals:

$$\begin{aligned} a(\beta_1 u_1 + \beta_2 u_2, v) &= \int_0^1 \alpha(\beta_1 u_1 + \beta_2 u_2)_x v_x - b(\beta_1 u_1 + \beta_2 u_2)v_x + c(\beta_1 u_1 + \beta_2 u_2)v\, dx \\ &= \beta_1 \int_0^1 \left(\alpha(u_1)_x v_x - bu_1 v_x + cuv\right)\, dx + \beta_2 \int_0^1 \left(\alpha(u_2)_x v_x - bu_2 v_x + cuv\right)\, dx \\ &= \beta_1 a(u_1, v) + \beta_2 a(u_2, v) \end{aligned}$$

For some constants β_1, β_2. Using similar arguments one can show that this also holds for the other input v, which shows that $a(u,v)$ is bilinear. Further, we know from functional analysis that for a bilinear mapping $B : X \times Y \longrightarrow Z$ on a normed vector space, the following assertions are equivalent: (i) B is continuous, (ii) B is bounded. That is, $\exists c \geq 0$ s.t. $\|B(x,y)\|_Z \leq C\|x\|_X\|y\|_Y \quad \forall \quad (x,y) \in X \times Y$.

In the next section we will use the fact that $a(u,v)$ is bilinear to show that it is bounded and thus also continuous. The Cauchy Schwarz inequality (C.S) $|\langle u, v\rangle| = \|u\|\|v\|$ will be used here and also elsewhere in the project.

$$\begin{aligned}
&|a(u,v)| = |\int_0^1 \alpha u_x v_x - buv_x + cuv \, dx| \\
&\leq |\int_0^1 \alpha u_x v_x dx| + |\int_0^1 buv_x dx| + |\int_0^1 cuv dx| \\
&\overset{C.S}{\leq} \|\alpha u_x\|_{L^2}\|v_x\|_{L^2} + \|bu\|_{L^2}\|v_x\|_{L^2} + \|cu\|_{L^2}\|v\|_{L^2} \\
&\leq \|\alpha\|_\infty\|u_x\|_{L^2}\|v_x\|_{L^2} + \|b\|_\infty\|u\|_{L^2}\|v_x\|_{L^2} + \|c\|_\infty\|u\|_{L^2}\|v\|_{L^2} \\
&\leq \|u\|_{H^1}\|v\|_{H^1}\left(\|\alpha\|_\infty + \|b\|_\infty + \|c\|_\infty\right) \leq \|u\|_{H^1}\|v\|_{H^1}K
\end{aligned} \tag{5}$$

Where we in the last line use the definition $\|u\|^2_{H^1} := \|u\|^2_{L^2} + \|u_x\|^2_{L^2}$, which shows $\|u\|_{L^2} \leq \|u\|_{H^1}$ and similarly also for u_x, v and v_x. This proves that $a(u,v)$ is bounded and thus also continuous.

Next we want to show that $F(v)$ is a linear continuous functional on H^1. First we show the linearity of $F(v)$ by $F(\lambda(v+u)) = \int_0^1 f\lambda(v+u)\,dx = \lambda F(v) + \lambda F(u)$ for some constant λ.

Further, from Riesz representation theorem we know that any normed space has a dual space of bounded/continuous linear functionals with norm $\|f\| := \sup_{\|x\|\neq 0} \dfrac{\|f(x)\|}{\|x\|_X}$. In this case we have

$$\|F\| = \max_{v\neq 0 \in H_0^1} \frac{|F(v)|}{\|v\|_{H^1}} = \max_{v\neq 0 \in H_0^1} \frac{|\int_0^1 fv \, dx|}{\|v\|_{H^1}} = \max_{v\neq 0 \in H_0^1} \frac{|\langle f, v\rangle|}{\|v\|_{H^1}} \overset{(C.S)}{\leq} \max_{v\neq 0 \in H_0^1} \frac{\|f\|_{L^2}\|v\|_{L^2}}{\|v\|_{H^1}} \leq \|f\|_{L^2} < \infty \tag{6}$$

$\implies$ $F(v)$ is bounded.

2.2 Existence of solution

In the next section we want to prove existence of solution u in (2) in the case where α, b, c are nonzero constants. We start by showing that $a(u,v)$ satisfies the Gårding inequality:

$$a(u,u) \geq (\alpha - \frac{\epsilon}{2}|b|)\int_0^1 u_x^2 dx + (c - \frac{1}{2\epsilon}|b|)\int_0^1 u^2 dx \qquad \forall \epsilon > 0 \tag{7}$$

with

$$a(u,u) = \int_0^1 \alpha u_x^2 - buu_x + cu^2 dx = \alpha\|u_x\|^2_{L^2} + c\|u\|^2_{L^2} - b\langle u, u_x\rangle.$$

We introduce notation to simplify expressions:

$$\int_0^1 u_x^2 dx = \|u_x\|^2_{L^2} := \beta^2 \ , \ \int_0^1 u^2 dx = \|u\|^2_{L^2} := \gamma^2$$

Modifying the RHS of (7), using Young's inequality $ab \leq \frac{1}{2\epsilon}a^2 + \frac{\epsilon}{2}b^2 (Yng)$ we obtain:

$$\begin{aligned}
\alpha\beta^2 - \frac{\epsilon}{2}|b|\beta^2 + c\gamma^2 - \frac{1}{2\epsilon}\gamma^2|b| &= \alpha\beta^2 + c\gamma^2 - |b|(\frac{1}{2\epsilon}\gamma^2 + \frac{\epsilon}{2}\beta^2) \\
&\overset{(Yng)}{\leq} \alpha\beta^2 + c\gamma^2 - \gamma\beta|b| \\
&= \alpha\|u_x\|^2_{L^2} + c\|u\|^2_{L^2} - |b|\|u_x\|_{L^2}\|u\|_{L^2} \overset{(C.S)}{\leq} a(u,v)
\end{aligned}$$

Further, we want to use this fact to show the coercivity of $a(u,v)$. We set $\epsilon = \frac{\alpha}{|b|}$ and obtain

$$\begin{aligned} a(u,u) &\geq (\alpha - \frac{\alpha}{2}) \int_0^1 u_x^2 dx + (c - \frac{|b|^2}{2\alpha}) \int_0^1 u^2 dx \\ &= \frac{\alpha}{2} \|u_x\|_{L^2}^2 + (c - \frac{|b|^2}{2\alpha}) \|u\|_{L^2}^2 \geq \delta \|u\|_{H^1}^2 \Rightarrow \ a(u,v) \text{ coercive conditional on } c > \frac{|b|^2}{2\alpha} \end{aligned}$$

Finally, we can see from the Lax-Milgram theorem (see Appendix B) that we have proven continuity $a(u,v) \leq M\|u\|_{H^1}\|v\|_{H^1}$ with continuity constant $M = K$ and coercivity $a(u,v) \geq \delta \|u\|_{H^1}^2$ with coercivity constant $\delta = \min\{\frac{\alpha}{2}, c - \frac{|b|^2}{2\alpha}\}$. From the Lax-Milgram theorem we therefore conclude that there exists a unique solution u to (2).

3 Part 2: $\mathbb{P}_1$ FEM on (0,1)

In the second part we let $\alpha, c > 0, b$ be nonzero constants. We want to solve problem (2) with a $\mathbb{P}_1$ FEM on a general grid on (0,1):

$$\text{find } u \in V_h \text{ s.t } a(u_h, v_h) = F(v_h) \quad \forall v_h \in V_h = X_h^1(0,1) \cap H_0^1(0,1) \tag{8}$$

where V_h is the space of continuous functions with zero boundary values, that are piecewise linear on the triangulation given by the grid. We define a partition $0 = x_0 < x_1 < ... < x_M = 1$ and elements $K_i := (x_{i-1}, x_i)$, $i = 1, ..., M$. We can then define the triangulation as $T_h := \{K_i\}_{i=1}^M$ and stepsizes $h_i := x_i - x_{i-1}$.

3.1 Derivation and implementation

The fundamental idea of FEM is to approximate the functions u in the infinite-dimensional space V by $u_h \in V_h$ where $V_h \subset V$ is some finite-dimesional space. If in addition we define a basis for V_h s.t. $\text{span}\{\phi_i\}_{i=0}^M = V_h$, expanding u_h and v_h in terms of this basis will lead to a linear system of equations. The function $\phi_i \in \mathbb{P}_1$, $i = 0, 1, ..., M$ evaluates to 1 at point x_i and 0 at all other grid points.

More precisely ϕ_i and its gradient ϕ_i' are defined as:

$$\phi_i(x) = \begin{cases} \frac{x - x_{i-1}}{x_i - x_{i-1}} & x_{i-1} < x \leq x_i \\ \frac{x_{i+1} - x}{x_{i+1} - x_i} & x_i < x \leq x_{i+1} \\ 0 & \text{otherwise} \end{cases} \qquad \phi_i'(x) = \begin{cases} \frac{1}{x_i - x_{i-1}} & x_{i-1} < x \leq x_i \\ -\frac{1}{x_{i+1} - x_i} & x_i < x \leq x_{i+1} \\ 0 & \text{otherwise} \end{cases}$$

$i = 1, ..., M-1$. Note that we did not define ϕ_0 or ϕ_M in this case since they will not be needed in the linear system we will solve. This will become clear later. As $u_h, v_h \in V_h$, we expand them in terms of the basis:

$$u_h(x) = \sum_{i=0}^M u(x_i)\phi_i(x), \quad v_h(x) = \sum_{j=0}^M v(x_j)\phi_i(x), \quad (u_h)_x(x) = \sum_{i=0}^M u(x_i)\phi_i'(x), \quad (v_h)_x(x) = \sum_{j=0}^M v(x_j)\phi_j'(x)$$

Using this, we can write (8) in the following linear system:

$$\sum_{i=0}^M u(x_i) \sum_{j=0}^M v(x_j) \int_0^1 \alpha \phi_i' \phi_j' - b\phi_i \phi_j' + c\phi_i\phi_j \, dx = \sum_{j=0}^M v_j \int_0^1 f\phi_j \, dx$$

$\Rightarrow v^T A u = v^T F \iff Au = F$. Where A is called the stiffness matrix. Note that since $u_h(0) = u_h(1) = 0$, we can restrict the problem further and solve for $i, j = 1, ..., M-1$. We observe that the product $\phi_i\phi_j$ is non-zero only if $j = i$ or $j = i \pm 1$. The same goes for the products $\phi_i\phi_j'$

and $\phi_i^{'}\phi_j^{'}$. We can then calculate the stiffness matrix $A = (a_{ij})_{i=1}^{M-1}$ and RHS F_j, $j = 1, ..., M-1$ elementwise:

$$A_{ij} = \int_0^1 \alpha\phi_i'\phi_j' - b\phi_i\phi_j' + c\phi_i\phi_j \, dx = \sum_K \int_{K_i} \alpha\phi_i'\phi_j' - b\phi_i\phi_j' + c\phi_i\phi_j \, dx$$

$$F_j = \int_0^1 f\phi_j \, dx = \sum_K \int_{K_i} f\phi_j \, dx$$

For the stiffness matrix A, we do the integration on the intervals $j = i$, $j = i \pm 1$:

$$\sum_{K_i} \int_0^1 \phi_i'\phi_j' \, dx = \begin{cases} -\frac{1}{h_i} & j = i-1 \\ \frac{1}{h_i} + \frac{1}{h_{i+1}} & j = i \\ -\frac{1}{h_{i+1}} & j = i+1 \end{cases} \quad \sum_{K_i} \int_0^1 \phi_i\phi_j' \, dx = \begin{cases} \frac{1}{2} & j = i-1 \\ 0 & j = i \\ -\frac{1}{2} & j = i+1 \end{cases} \quad \sum_{K_i} \int_0^1 \phi_i\phi_j' \, dx = \begin{cases} \frac{h_i}{6} & j = i-1 \\ \frac{h_i}{3} + \frac{h_{i+1}}{3} & j = i \\ \frac{h_{i+1}}{6} & j = i+1 \end{cases} \tag{9}$$

We compress these results into the vectors for subdiagonal $\vec{\sigma}_i := \left(-\frac{1}{h_i}, \frac{1}{2}, \frac{h_i}{6}\right)^T$, main diagonal $\vec{\beta}_i := \left(\frac{1}{h_i} + \frac{1}{h_{i+1}}, 0, \frac{h_i}{3} + \frac{h_{i+1}}{3}\right)^T$ and supdiagonal $\vec{\gamma}_i := \left(-\frac{1}{h_{i+1}}, -\frac{1}{2}, \frac{h_{i+1}}{6}\right)^T$ for $j = i-1, \ i, \ i+1$ respectively. We also define $\vec{r} := (\alpha, -b, c)$. Because of the Dirichlet boundary condition on u we remove first/last row/column from A, and we write (inner) $A \in R^{(M-2)\times(M-2)}$ as

$$A_{inner} = \begin{bmatrix} \vec{r}\vec{\beta}_2 & \vec{r}\vec{\gamma}_2 & & & \\ \vec{r}\vec{\sigma}_3 & \vec{r}\vec{\beta}_3 & \vec{r}\vec{\gamma}_3 & & \\ & \ddots & \ddots & \ddots & \\ & & \vec{r}\vec{\sigma}_{M-2} & \vec{r}\vec{\beta}_{M-2} & \vec{r}\vec{\gamma}_{M-2} \\ & & & \vec{r}\vec{\sigma}_{M-1} & \vec{r}\vec{\beta}_{M-1} \end{bmatrix}$$

To solve for the RHS F_j we will use a numerical quadrature method s.t. $F_j = \int_0^1 f\phi_j dx \approx Q_{[0,1]} f\phi_j$. In this project we will use both scipy functions **integrate.quad()** and **integrate.simpson()**, which are implementations of Gaussian quadrature and Simpsons method respectively. They will ensure sufficient convergence rate for the FEM (order 2).

3.2 Testing numerical scheme

We implement two test functions with exact solutions u_1 and u_2 and with RHS f_1 and f_2 respectively:

$$u_1(x) = x(1-x), \quad f_1(x) = 2\alpha + b(1-2x) + cx(1-x)$$

$$u_2(x) = \sin(3\pi x), \quad f_2(x) = 9\alpha\pi^2\sin(3\pi x) + 3b\pi\cos(3\pi x) + c\sin(3\pi x)$$

In the first part of the testing we set the coefficients $\alpha, b, c = 1$. In Figure 1 we see an interesting case of the stiffness matrix A_{inner} with the gridpoints $x = (0, 0.1, 0.3, 0, 5, 0.6, 0.8, 0.9, 0.95, 0.97, 1)$, where the (inner) gridpoints are chosen randomly.

15.1	-4.46667	0	0	0	0	0	0	0
-5.46667	1.63333	3.78333	0	0	0	0	0	0
0	2.78333	-1.56667	1.13333	0	0	0	0	0
0	0	0.133333	0.172727	-0.00606061	0	0	0	0
0	0	0	-1.00606	3.37273	-4.46667	0	0	0
0	0	0	0	-5.46667	15.1	-9.48333	0	0
0	0	0	0	0	-10.4833	30.05	-19.4917	0
0	0	0	0	0	0	-20.4917	70.0233	-49.4967
0	0	0	0	0	0	0	-50.4967	83.35

Figure 1: Stiffness matrix

Next we look at the convergence rates in $\|\cdot\|_{L^2}$ and $\|\cdot\|_{H^1}$ for our scheme on the two test functions when **Simpson** is used. We test it by computing the solutions on equidistant grid points while iteratively doubling the number of nodes (starting with 10) in the triangulation. For each iteration we compute the error $\|u - u_h\|$ (by **Simpson**) in each respective norm, where u is the exact

solution. We use log-log plots to see the order of convergence of the two methods. The result can be seen in Figure 2, along with a theoretical error bound in the H^1-norm which is given by $\|u - u_h\|_{H^1} \leq \frac{2Mh}{\delta}\|u_{xx}\|_{L^2}$. Here $M = \alpha + |b| + c + \|f\|_{L^2}$ and $\delta = \frac{\alpha}{2}$. For proof, see section 3.3.

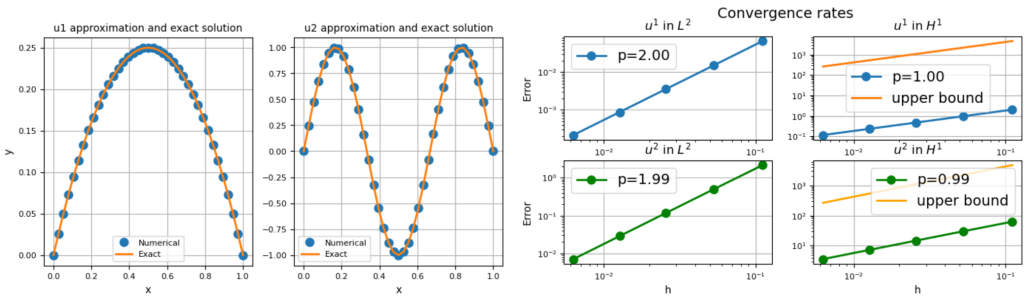

$u_1 = x(1-x), u_2 = \sin 3\pi x$ Convergence rates for u_1 and u_2 in L^2 and H^1

Figure 2: Analysis of u_1 and u_2

We can see that both methods show order of convergence 2 in $\|\cdot\|_{L^2}$ and order 1 in $\|\cdot\|_{H^1}$ with maximum error in order of less than 10^1 and 10^2 in the H^1-norm for u_1 and u_2 respectively. Both functions are well below the theoretical upper bound in H^1, which should not be surprising since the bound is not very tight. In the figure we can also see the approximations of the two methods plotted with their respective analytic solutions. From the plots it seems like the test functions are good approximations, which compliments the result in the convergence plots.

3.3 Galerkin orthogonality and Cea's lemma

In this section we will show Galerkin orthogonality for the $\mathbb{P}_1$ FEM (V_h). In addition we will show that Cea's Lemma holds for this problem and find an H^1 error bound.

Lemma: *(Galerkin orthogonality) Let u and u_h be the solutions of the infinite and finite dimensional variational problems respectively. Then*

$$a(u - u_h, v_h) = 0 \quad \forall v \in V_h$$

Lemma: *(Cea's lemma) Let u and u_h be the solutions of the infinite and finite dimensional variational problems respectively, and supposse that the hypotheses of Lax-Milgram theorem are satisfied. Notably, we assume that a is continuous and coercive with constants M and α. Then*

$$\|u - u_h\|_V \leq \frac{M}{\alpha}\|u - v_h\|_V \quad \forall v_h \in V_h$$

Galerkin orthogonality for (V_h):

$V_h = X_h^1(0,1) \cap H_0^1(0,1) \quad X_h^1 = \{v_h \in C(\overline{\Omega}) : v_h|_K \in \mathbb{P}_1 \ \forall K \in T_h\}$ Triangulation: $T_h = \{K_i\}_{i=1}^M$

With $\overline{\Omega} = [0,1]$ in this case. Because of bilinearity we have

$$a(u - u_h, v_h) = a(u, v_h) - a(u_h, v_h) = F(v_h) - F(v_h) = 0$$

since $v_h \in V_h \subset V$ and $a(u, v_h) = F(v_h) = a(u_h, v_h)$. $\square$

To show that Cea's lemma holds for this problem, it suffices to show that the problem is coercive and continuous according to the Lax-Milgram theorem. We did this in the infinite dimensional case, and as $V_h \subset V$, we come to the same conclusion, and we conclude that Lax-Milgram also holds for $a(u_h, v_h)$. Therefore Cea's lemma holds for this problem.

Next we look to prove the H^1 error bound stated in section 3.2. From Cea's lemma we have

$$\|u - u_h\|_{H^1} \leq \frac{M}{\alpha}\|u - v_h\|_{H^1} \quad \forall v_h \in V_h$$

Where M is the continuity constant and α the coercivity constant. Since we have already used the notation for α, we change this notation: $\alpha \to \delta$. By Galerkin orthogonality, we have $a(u-u_h, w_h) = 0 \quad \forall w_h \in V_h$. We choose $w_h := u_h - v_h \in H_0^1$:

$$\delta\|u-u_h\|_{H^1}^2 \leq a(u-u_h, u-u_h) = a(u-u_h, u-u_h) + a(u-u_h, u-v_h) \leq M\|u-u_h\|_{H^1}\|u-v_h\|_{H^1}$$

$$\implies \|u-u_h\|_{H^1} \leq \tfrac{M}{\delta}\|u-v_h\| \quad \forall v_h \in H_0^1$$

which we can see is equivalent to the expression in Cea's lemma. We can use this to provide an error bound in H^1, using the interpolant error estimate in L^2-norm given by $\tilde{E}_h(v) \leq 2h\|v_{xx}\|_{L^2(0,1)}$:

$$\|u - u_h\|_{H^1} \leq \frac{2Mh}{\delta}\|u_{xx}\|_{L^2(0,1)}$$

We see that the error bound is of order 1, which agrees with our analysis of u_1 and u_2 seen in Figure 2

3.4 Non-smooth exact solutions

In this section we will discuss two non-smooth exact solutions w_1 and w_2. We will show that both functions belong to $H^1(0,1)$ but not to $H^2(0,1) := \{g : g, g_x, g_{xx} \in L^2(0,1)\}$. We define the functions:

$$w_1(x) = \begin{cases} 2x, & x \in (0, \frac{1}{2}) \\ 2(1-x), & x \in (\frac{1}{2}, 1) \end{cases} \qquad \text{and} \qquad w_2(x) = x - |x|^{\frac{2}{3}}. \tag{10}$$

These functions are not (strongly) differentiable at $x = \frac{1}{2}$ and $x = 0$ respectively, as they are discontinuous in these points. In this section we will discuss differentiability in the weak sense. We state the definition of the weak derivative in this case. For a function $u(x)$, $u'(x) = u_x$ is a weak derivative if the following holds:

$$\int_0^1 u_x v dx = -\int_0^1 u v_x dx, \quad \forall v \in H_0^1(0,1), \quad \text{and} \quad u_x \in L^2(0,1)$$

We start by checking the function w_1:

$$\begin{aligned} \int_0^1 w_1' v dx &= [w_1 v]_0^1 - \int_0^1 w_1 v_x dx \\ &= -\int_0^{\frac{1}{2}} 2x v_x dx - \int_{\frac{1}{2}}^1 2(1-x) v_x dx \\ &= -\int_0^1 w_1 v_x dx \end{aligned}$$

and since $w_1' = \begin{cases} 2, & x \in (0, \frac{1}{2}) \\ -2, & x \in (\frac{1}{2}, 1) \end{cases}$ is constant on the interval $[0,1]$, it clearly converges in $L^2(0,1)$, showing that it is a weak derivative of w_1. Further, since w_1 is a piecewise polynomial on $[0,1]$, we know that it also converges in the L^2-norm. Thus we have showed $w_1 \in H^1(0,1)$. Next, we show

that $w_1 \notin H^2(0,1)$. We start by looking for w_1'':

$$\begin{aligned}
\int_0^1 w_1'' v dx &= [w_1' v]_0^1 - \int_0^1 w_1' v_x dx \\
&= -\int_0^{\frac{1}{2}} 2 v_x dx - \int_{\frac{1}{2}}^1 -2 v_x dx \\
&= 4v(\frac{1}{2}) \\
&\neq -\int_0^1 w_1' v_x dx \quad \forall v \in H^1(0,1) \\
&\implies w_1' \notin H_0^1 \iff w_1 \notin H^2(0,1)
\end{aligned}$$

Next we look at w_2 which is equal to $x - |x|^{\frac{2}{3}}$ on the interval $[0,1]$. We look for the existence of $w_2' = 1 - \frac{2}{3}|x|^{-\frac{1}{3}}$:

$$\int_0^1 w_2' v dx = \underbrace{[w_2 v]_0^1}_{=0} - \int_0^1 w_2 v_x dx = -\int_0^1 w_2 v_x dx \quad \forall v \in H_0^1(0,1)$$

We see that w_2' exists. Further, we see that $\|w_2\|^2_{L^2(0,1)} = \frac{1}{84}$ converges in $L^2(0,1)$. Also, $\|w_2'\|^2_{L^2(0,1)} = \frac{4}{9}[3x^{\frac{1}{3}}]_0^1$ converges. Using the same procedure by the definiton of weak derivative as for w_2', we can find a function $w_2'' = \frac{2}{9}|x|^{-\frac{4}{3}}$. However we find that $\|w_2''\|^2_{L^2} = \frac{4}{81}[\frac{2}{9}x^{-\frac{5}{3}}]_0^1$ diverges, which means that w_2'' can not be a weak derivative of w_2'. Finally this shows us that $w_2 \in H^1(0,1)$ but $w_2 \notin H^2(0,1)$.

We move on to test the convergence rates of w_1 and w_2 using the same procedure as for the functions u_1 and u_2. Since we have found that w_{xx} does not exist (even in the weak sense) for both w_1 and w_2, we transform these terms on the RHS of (8) with ibp.: $\int_0^1 w_{xx}\phi_i dx = -\int_0^1 w_x \phi_i' dx$. The problem will then be well defined. A plot of the convergence rates can be seen below in Figure 3.

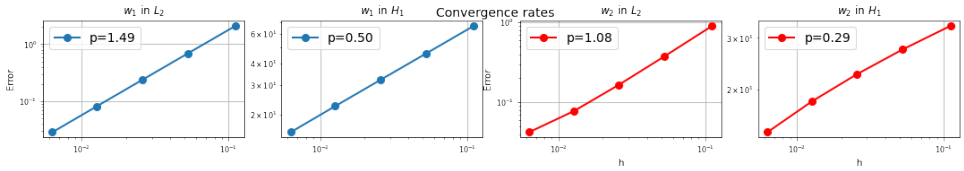

Figure 3: Convergence rates for w_1 and w_2 in $L^2(0,1)$ and $H^1(0,1)$

The plots confirm the over all decrease in order for w_1 and w_2 compared to u_1 and u_2. This should not be a surprise given their discontinuity at $x = \frac{1}{2}$ and $x = 0$ respectively. The biggest decrease in order is seen in H^1-norm for w_2. This can be explained by the term w_2' which goes to infinity as x goes to zero, which will affect the error in H^1. In the convergence plots we have only used equidistant grid points. One advantage of the FEM is that we can pick the triangulation. On the left in Figure 3 in Appendix A we can see the numerical solution of w_1 plotted with it's analytic solution with 15 nodes, inner nodes chosen at random. Choosing more nodes near singularities can help decrease the error, as seen on the right in Figure 3 where two solutions of w_2 is plotted. With the same amount of nodes, we plot one solution with equispaced nodes while the other has more points near the singularity at $x = 0$. By test of the eye, we can clearly see that the solution with more nodes near zero is a better approximation compared to the one with equidistant nodes. We explore this further in section 3.5.

3.5 Different placements of nodes

In this final section of the project we want to analyze the impact of the placement of nodes for an analytic function that is rapidly growing in some area. We will work with no analytic solution,

but only the RHS function

$$f_5(x) = x^{-\frac{1}{4}} \in L^2(0,1)$$

First we confirm that $f_5 \in L^2(0,1)$. We have

$$\|f_5\|_{L^2(0,1)} = (\int_0^1 (x^{-\frac{1}{4}})^2 dx)^{0.5} = \sqrt{2} \implies \text{converges} \implies f_5 \in L^2(0,1)$$

Since we do not have an analytic function to compare to, we will use a very refined numerical solution, namely one with 1000 equispaced nodes. We will be using the scipy function **integrate.quad()** for all methods in this section. In addition we will update the parameters s.t. $\alpha, b, c = 1, -5, 14$ in this final part. We will implement two test solutions to compare with our "analytic" solution u_5. To have a fair comparison, we will use the same amount of nodes, 15. One solution will have equispaced grid points while the other will have more grid points near the rapidly growing area at around $x = 0$. We call these grid points x_1 and x_2 respectively (see Appendix B).

We test the error in $\|u_5 - u_h\|_{L^2}$ for the two methods, with resulting error of 0.000523 for the case of nodes x_1 and 0.000271 for the case of nodes x_2 as seen in Figure 5 in Appendix A. Both methods perform rather well, however as expected the error is smaller for the method with more nodes near 0, which shows one of the main features of the FEM, which allows us to place more nodes where the function values change rapidly and improve the accuracy of the method.

Appendix

A Figures

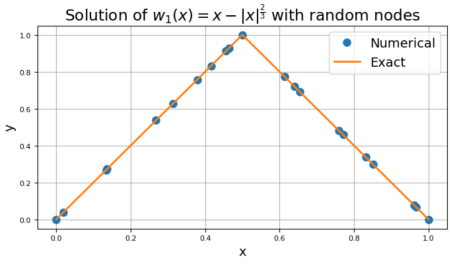

w_1 with random nodes

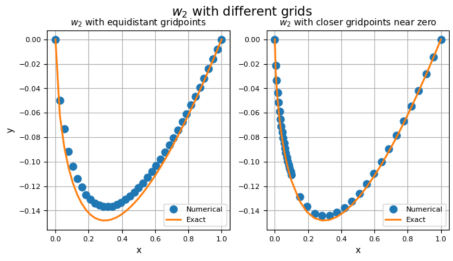

w_2 with equispaced nodes and more nodes near zero

Figure 4: Plots of non-smooth functions

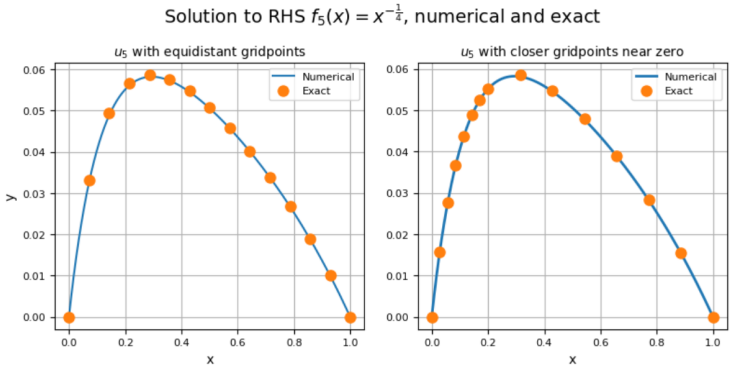

Solution to f_5 with equispaced nodes and more nodes near zero

```
Error for equidistant:  0.0005232592796499337

Error for closer near zero:  0.00027191257863051733
```

Error $\|u_5 - u_h\|_{L^2}$ for equispaced nodes and more nodes near zero

Figure 5: Analysis of f_5

B Additional information

Theorem (Lax-Milgram)**.** *Let V be a Hilbert space. Suppose that F is a continuous linear functional (it suffices that F be bounded), and that a is a continuous, coercive bilinear form, i.e. there exists M, δ such that*

(1) (Continuous) $a(u, v) \leq M\|u\|_V\|v\|_V$ for all $u, v \in V$

(2) (Coercive) $a(u, u) \geq \delta\|u\|_V^2$ for all $v \in V$

Then the variational problem: find $u \in V$ such that, for all $v \in V$,

$$a(u, v) = F(v)$$

admits a unique solution

Grids used in section 3.5 Different placements of nodes. x_1 is equispaced while x_2 has more nodes near $x = 0$.

$x_1 = (0, 0.071, 0.142, 0.214, 0.285, 0.357, 0.428, 0.5, 0.571, 0.642, 0.714, 0.785, 0.857, 0.928, 1)$

$x_2 = (0, 0.028, 0.056, 0.085, 0.113, 0.141, 0.17, 0.2, 0.314, 0.428, 0.542, 0.657, 0.771, 0.885, 1)$